

The Uses and Limitations of the Square-Root-Impedance Method for Computing Site Amplification

by David M. Boore

Abstract The square-root-impedance (SRI) method is a fast way of computing approximate site amplification that does not depend on the details from velocity models. The SRI method underestimates the peak response of models with large impedance contrasts near their base, but the amplifications for those models is often close to or equal to the root mean square of the theoretical full resonant (FR) response of the higher modes. On the other hand, for velocity models made up of gradients, with no significant impedance changes across small ranges of depth, the SRI method systematically underestimates the theoretical FR response over a wide frequency range. For commonly used gradient models for generic rock sites, the SRI method underestimates the FR response by about 20%–30%. Notwithstanding the persistent underestimation of amplifications from theoretical FR calculations, however, amplifications from the SRI method may often provide more useful estimates of amplifications than the FR method, because the SRI amplifications are not sensitive to details of the models and will not exhibit the many peaks and valleys characteristic of theoretical full resonant amplifications (jaggedness sometimes not seen in amplifications based on averages of site response from multiple recordings at a given site). The lack of sensitivity to details of the velocity models also makes the SRI method useful in comparing the response of various velocity models, in spite of any systematic underestimation of the response. The quarter-wavelength average velocity, which is fundamental to the SRI method, is useful by itself in site characterization, and as such, is the fundamental parameter used to characterize the site response in a number of recent ground-motion prediction equations.

Introduction

The square-root-impedance (SRI) method provides a rapid way of computing approximate linear site amplifications. The amplifications are not sensitive to details of the velocity model (e.g., [Anderson *et al.*, 1996](#)), and in addition, [Day \(1996\)](#) shows that a spectral average of the amplification is not dependent on the velocity structure below a well-defined, frequency-dependent depth. The method is widely used for computing amplifications in simulations of ground motions (e.g., [Boore and Joyner, 1997](#); [Boore, 2003](#)) and as a means of comparing different estimates of seismic velocity beneath a single site (e.g., [Brown *et al.*, 2002](#); [Stephenson *et al.*, 2005](#)).

Although widely used, the method only provides an approximation to the site amplification computed from theoretical simulations of wave propagation in layered media that account for the constructive and destructive interference of all reverberations in the layers (what I call here “full resonant amplifications”, or FR amplifications). A few comparisons of SRI amplifications and FR amplifications have appeared in the literature (e.g., [Boore and Joyner, 1991](#); [Douglas *et al.*, 2009](#)), but these studies did not focus on a comparison of the

SRI and FR amplifications for a wide range of velocity models. The studies did show, however, that the SRI method has apparent limitations: It always underestimates the amplitude of the fundamental mode of a resonant system, and it also underestimates the response even for gradient profiles, with no impedance changes across layers. The purpose of this note is to draw attention to the method and its possible limitations, with a discussion of when it might be useful and when it should be used with caution. The next section discusses the method, and the following section contains comparisons of SRI and FR site response for a variety of models, ranging from simple layered systems with large changes in seismic impedance between layers to gradient models without and with impedance contrasts. The amplifications in most of these examples are computed assuming no attenuation in the model. I then include a brief comparison of amplifications computed with attenuation. This is followed by a section discussing uses of the SRI method.

The basis for the conclusions in this paper is the comparison of theoretical site response computed using the SRI and FR methods. It is tempting to call the FR response the

true response, but this would be wrong. A number of studies have found moderate-to-poor comparisons between the observed site response and the FR site response for sites with well determined velocity models, even for models for which lateral changes in velocity are expected to be small compared to the vertical changes (e.g., see the review by Boore, 2004, and more recent comparisons, such as Thompson *et al.*, 2009). The accuracy of theoretical FR site-specific predictions of site response is well beyond the scope of this paper, which is to review the SRI method and to compare the approximate theoretical amplifications with those from the mathematically more exact FR calculations. The resulting amplifications from either method should be taken as approximations of the true amplification.

The Square-Root-Impedance Method

Ray theory predicts that the amplitude of motion along a ray tube will be inversely proportional to the square root of local seismic impedance Z , for which $Z = \rho V$, with ρ and V being density and seismic wave propagation velocity, respectively (e.g., equation 4.62 in Aki and Richards, 2002). Wiggins (1964) observed that the response at the surface of a single constant-velocity layer relative to the surface motion of a half-space formed by removing the layer was similar to the ratio of the square root of the seismic impedances of the half-space and the layer. Joyner *et al.* (1981) extended this idea in several important ways. They proposed that the site amplification A for an arbitrary velocity model be given by

$$A = \left(\frac{Z_R}{\bar{Z}}\right)^{1/2} \left(\frac{\cos \Theta_R}{\cos \bar{\Theta}}\right)^{1/2} = \left(\frac{\rho_R V_R}{\bar{\rho} \bar{V}}\right)^{1/2} \left(\frac{\cos \Theta_R}{\cos \bar{\Theta}}\right)^{1/2}, \quad (1)$$

for which ρ and V are density and seismic shear-wave velocity (usually written with a subscript S , but this is dropped here for clarity; I only consider shear waves in this paper), and Θ is the angle of incidence of the ray, relative to the vertical direction. The cosine term accounts for the projection of the cross sectional area in the ray tube onto the horizontal plane representing the free surface. The subscript R in equation (1) refers to properties at the reference depth, and the bars over the denominator variables indicate an average of the properties near the surface. Another innovation of Joyner *et al.* (1981) was in proposing that the average velocity be formed over a depth corresponding to one-quarter of a wavelength for each frequency being considered. They did not state the reasons for this choice, but it was probably because the fundamental-mode resonant frequency of a single layer with the depth and velocity given by their choice equals the frequency being considered. More detail regarding the computation of the averages can be found in Boore (2003), although in that article I inexplicably neglected the cosine terms; they are included, however, in my software program *site_amp* that computes the SRI site response. The effective

angle of incidence $\bar{\Theta}$ is computed, using Snell's law, by the following equation:

$$\bar{\Theta} = \sin^{-1}[(\bar{V}/V_R) \sin \Theta_R]. \quad (2)$$

I refer to the computation of site amplification using equation (1) as the SRI method. It is also sometimes known as the quarter-wavelength (QWL) method, but I prefer to use the term SRI for the site amplification part of the procedure, which uses QWL velocities and densities. Note that Joyner *et al.* (1981) estimated site amplifications using the SRI method, but in a later paper, Joyner and Fumal (1984, 1985) used the QWL computations to obtain average velocities for sites that had recorded strong motions and used these velocities to characterize each site in the development of ground-motion prediction equations (GMPEs). Joyner and Fumal did not use equation (1) directly in their analysis. In a similar application, Boore *et al.* (1994) used the velocity averaged to 30 m as the site variable, rather than a depth commensurate with the period of interest, because measured shear-wave velocities were available to that depth for more than half of the records used in their analysis. Since then, the time averaged velocity to 30 m (V_{S30}) has been widely used to characterize sites in recent GMPEs (and Boore *et al.*, 2011, show that V_{S30} correlates well with V_{S_z} , for averaging depths z both less than and much greater than 30 m).

The amplification A in equation (1) can be thought of as the amplitude along the ray tube, projected onto a plane representing the free surface, relative to the motion on a horizontal plane at the reference depth. Amplifications computed from equation (1) have been used in stochastic model simulations in which motions are computed at the earth's surface, starting from the source (e.g., Boore, 2003). In such applications an additional factor representing the effect of the free surface (usually a factor of 2, because plane SH waves are assumed) needs to be applied. The amplification A can also be thought of as the ratio of the motion at the free surface relative to the motion at the surface of a half-space formed by removing all material above the reference depth, assuming that the effect of the free surface is the same, so that it cancels out of the ratio. This is the sense in which A is used in this paper.

Attenuation in the SRI method is accounted for by multiplying the amplification in equation (1) by the operator

$$\exp(-\pi \kappa_0 f), \quad (3)$$

for which κ_0 is an attenuation parameter, which is usually determined empirically. κ_0 can also be given by the integral of travel time divided by the depth-dependent attenuation parameter Q over some portion of the travel path (e.g., Anderson *et al.*, 1996), but then care must be taken to separate that contribution to the diminution of the high frequency energy from the contribution produced by the whole-path Q operator usually used in the stochastic method.

Examples

In this section, I compare amplifications from the SRI method with those from FR calculations. The amplifications are defined as the ratio of the Fourier amplitude spectra of the motion at the surface of the velocity model and the motion that would have occurred at the surface of an equivalent constant-velocity half-space model in which the layers above the reference depth have been removed. The FR calculations assume plane *SH* waves. Unless stated otherwise, a vertical angle of incidence is assumed at the base of the velocity model.

For most of the comparisons the response was computed with no attenuation. I refer to those as “amplification” (even though the response can be less than unity), whereas the complete response including attenuation is perhaps better termed “site response”. I compare SRI and FR amplifications without attenuation because the usual procedure for using the SRI method is to first compute the no-attenuation amplifications and then apply the attenuation operator given by equation (3). Applying the same operator to the FR amplifications will result in the same ratio of FR to SRI amplifications as for the unattenuated amplifications. As discussed later, however, a better way of doing the full site response from the FR method is to include attenuation in each layer (through the parameter Q). As shown later, doing this is not exactly equivalent to applying the κ_0 operator given by equation (3), even when κ_0 is determined from the velocity and Q model. The difference in the FR site response, averaged over frequencies, for the two ways of incorporating the attenuation is relatively small, however, and thus for simplicity of comparing the FR and SRI amplifications I have used only the unattenuated response in most of the examples.

As a first example, I show a comparison from Boore and Joyner (1991). Figure 1 shows the velocity model and amplifications for models with and without a large change in velocity at 650 m. The amplifications were computed from frequency-domain calculations, using the programs *site_amp* and *nrattle* (see the Data and Resources section). Unlike most of the examples in this paper, there is attenuation in the site response in this example. For the FR calculations, attenuation is included by specifying constant Q values in each layer (see Boore and Joyner, 1991, for the values of Q); for the SRI amplifications, attenuation is included by using equation (3) with $\kappa_0 = 0.03$ s (the value for one passage through the model when Q is included). This example gives a preview of many things shown in subsequent examples. The first and least interesting observation is that the amplifications from both methods asymptotically approach unity at low frequencies, which is a necessary consequence of the ways in which the amplifications are computed. More interesting and important is that the SRI method underestimates the peaks of a resonant system, but it gives a good estimate of the average of the FR amplifications over a broad frequency range of the peaks and troughs. Finally, the SRI method underestimates

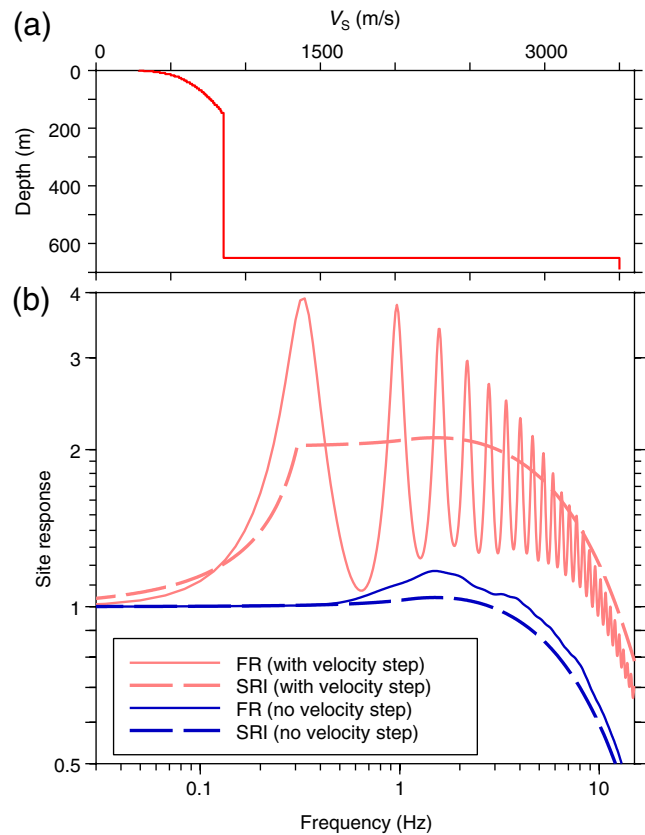


Figure 1. (a) Velocity model for a thick section of soils underlain by a high velocity half-space; (b) FR and SRI amplifications for a model with and without the step change in velocity at 650 m. The color version of this figure is available only in the electronic edition.

the FR response of gradient models with no impedance contrasts over a wide range of frequencies.

To aid in understanding how site resonances are built up from a series of reverberations, I obtained the impulse-response time series for the model with a velocity step shown in Figure 1. I computed the impulse response by using an inverse Fourier transform applied to the FR frequency-domain transfer function computed in the usual way (one of the output files of *nrattle* is the complex Fourier spectrum of the response, so that the proper phase of the response is retained). I then used Fourier spectra from portions of the impulse response that included the direct arrival, the direct arrival plus first reverberation, the direct arrival plus two reverberations, and so on. The impulse-response time series is shown in Figure 2a, and the site responses from the Fourier spectra of four progressively longer segments of the impulse response are shown in Figure 2b. The large impedance change in the model accentuates the amplitude of the later arrivals, but even so, it is clear that the later arrivals rapidly diminish in amplitude. Yet it is clear from Figure 2 that the full resonant response requires many of these later arrivals, even though their amplitudes are very small. The time spacing between sequential reverberations in this plane-layered model must be constant in order for complete constructive

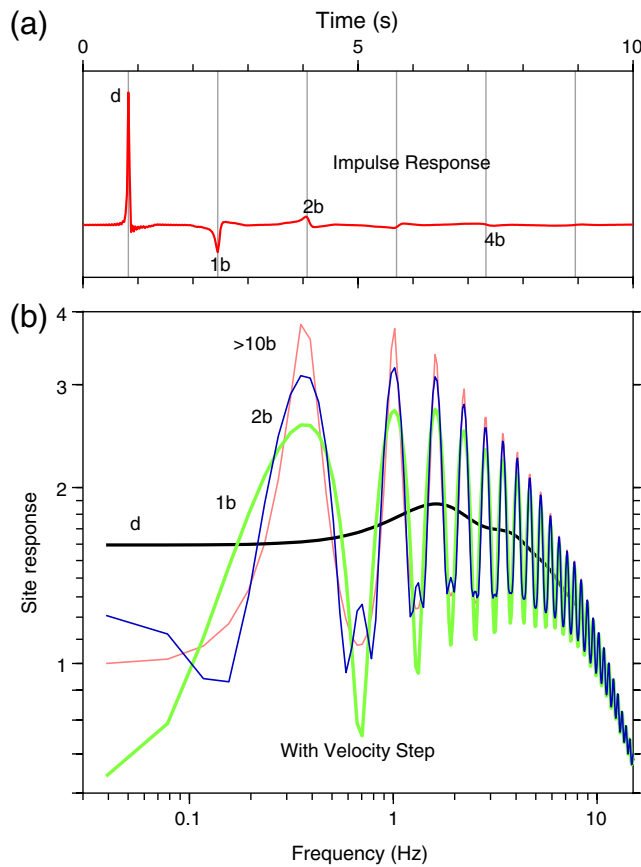


Figure 2. (a) The impulse response for vertically propagating SH waves in the soil column of the previous figure, using a modification of the program *nrattle* that includes all reverberations. Indicated are the direct arrival (d) and the arrivals that have made additional one, two, and four round trips through the entire soil column (1b, 2b, and 4b, respectively); the vertical gray lines indicate the times of the multiple arrivals; (b) The soil response, relative to a half-space without the soil column, obtained by computing the Fourier transform of the impulse response, windowed to include various numbers of multiple bounces (as indicated by the labels). (Modified from figs. A1 and A2 in [Boore and Joyner, 1991](#).) The color version of this figure is available only in the electronic edition.

and destructive interference to take place. In my view, it is unlikely that this will happen in reality because of lateral heterogeneities in the velocity structure, and nonlinear soil response may also lead to a reduction in the peaks, but this is another matter not considered here. For these reasons, I recommend that the peak resonant amplitudes shown in the subsequent examples be viewed with some skepticism. I am not disputing the presence of resonant peaks or the frequencies at which they occur, but by discounting to some extent the amplitudes of the FR peaks, the underestimation of the peaks by the SRI method will not be quite as severe as it appears in the examples for resonant systems.

Example of Models with Same Travel Time to Base

SRI and FR amplifications were computed for the set of velocity models shown in Figure 3 (the density was assumed

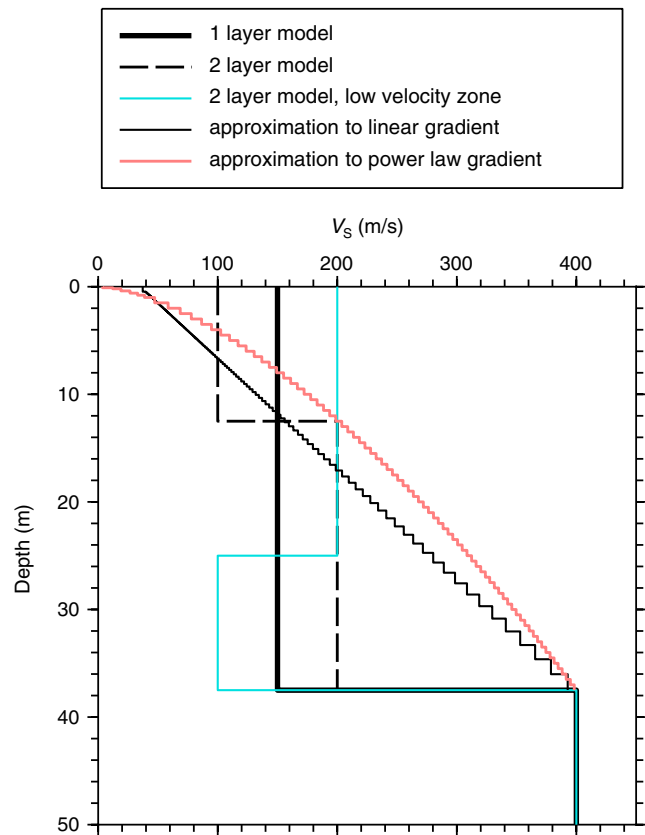


Figure 3. Five shear-wave velocity models, all of which have the same travel time (0.25 s) from the surface to the large impedance change at 37.5 m. The half-space below the interface at 37.5 m has a constant velocity of 400 m/s. The color version of this figure is available only in the electronic edition.

to be constant for all layers). These models include one- and two-layer models (the latter in two versions, one with the layers interchanged so as to create a low-velocity zone above the half-space), as well as models with linear and power-law gradients (with no impedance contrast at the interface between the upper part of the model and the half-space). All models have one thing in common: The travel time to the constant-velocity half-space at 37.5 m is the same (0.25 s). The amplifications relative to the half-space were computed using SRI and FR calculations, assuming vertically incident SH waves (using the program *nrattle*; see the [Data and Resources](#) section). As *nrattle* requires constant-velocity layers, the gradient models were replaced with models consisting of a stack of constant-velocity layers constructed so that the travel time to 37.5 m was the same as in the continuous gradient models (the program *site_amp* was used for this model construction). Figure 3 shows the models used in the computations, and Figure 4 shows the amplifications. Results are also shown for the 1-layer model with a 30° angle of incidence. As indicated in the upper left graph, the peaks of the resonant peaks for the 1-layer model are equal to the ratio of the impedances of the layer and the half-space, whereas the SRI amplitude is given by the square root of

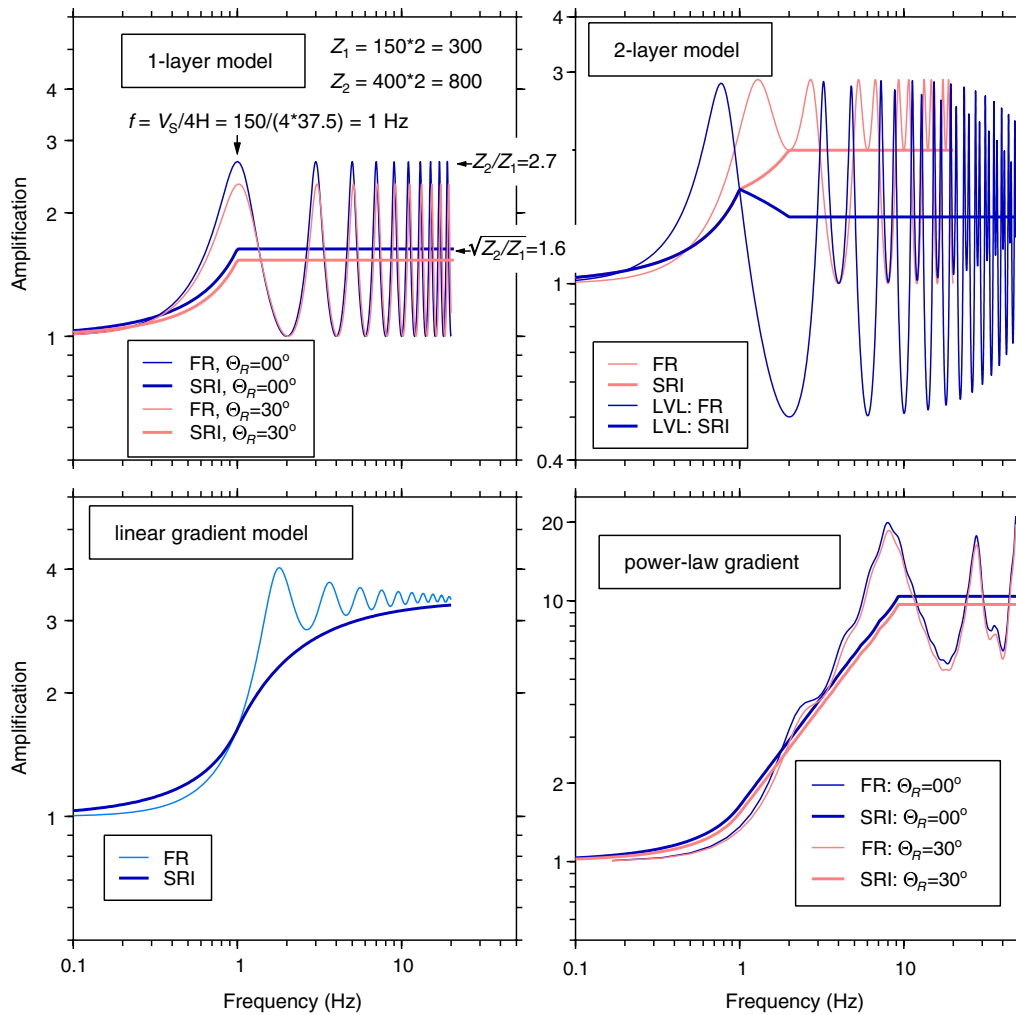


Figure 4. The amplifications for the five models shown in Figure 3, computed using the SRI method and FR calculations assuming vertically incident SH waves (Θ_R is the angle of incidence). The density was assumed to be constant, with a value of 2.0 g/cm^3 . The amplifications are relative to the motions at the surface of an effective half-space formed by removing the material above 37.5 m. There is no attenuation in the models. The color version of this figure is available only in the electronic edition.

the impedance ratio. For this model the SRI amplifications are exactly equal to the root mean square of the FR amplifications for frequencies greater than the fundamental mode, which occurs at 1 Hz, as indicated in Figure 4. Introducing another layer leads to complications in the response, such that the frequencies of the peaks of the FR response are no longer given by the simple rule-of-thumb that $f = V_{S_z}/4H$ and odd multiples thereof, for which V_{S_z} is the QWL velocity from the surface to the half-space. For both the 1- and 2-layer cases the amplitude of the fundamental resonant peak is underestimated by the SRI method. For the two gradient models, amplifications were computed for several approximations of the velocity models, which were made up of large numbers of constant-velocity layers to ensure that the observed oscillations and undulations in the FR amplifications for those models shown in Figure 4 are a feature of the gradient models and are not a consequence of the discretization of the continuous velocity structure (e.g.,

the amplification for the power-law model shown in Figure 3 used 600 layers, but virtually the same result was obtained when 1200 layers were used to approximate the continuous power-law model). All of the models, including the gradient models, exhibit pronounced resonant peaks and troughs, and these resonant peaks are always underestimated by the SRI amplifications. On the other hand, the SRI amplifications are close to or equal to the root mean square of the FR amplifications at frequencies above the fundamental mode for all but the linear gradient model. For that model, the SRI and FR amplifications approach one another only at very high frequencies. The relatively high frequency (near 10 Hz) at which the maximum amplification is reached in the power-law model is a result of the peculiar nature of that simple model, for which the velocity approaches 0.0 at the surface. The consequence is that the QWL frequency of the first layer, whose velocity and thickness are 3.7 m/s and 0.1 m (this thin layer was introduced at the surface to stabilize the

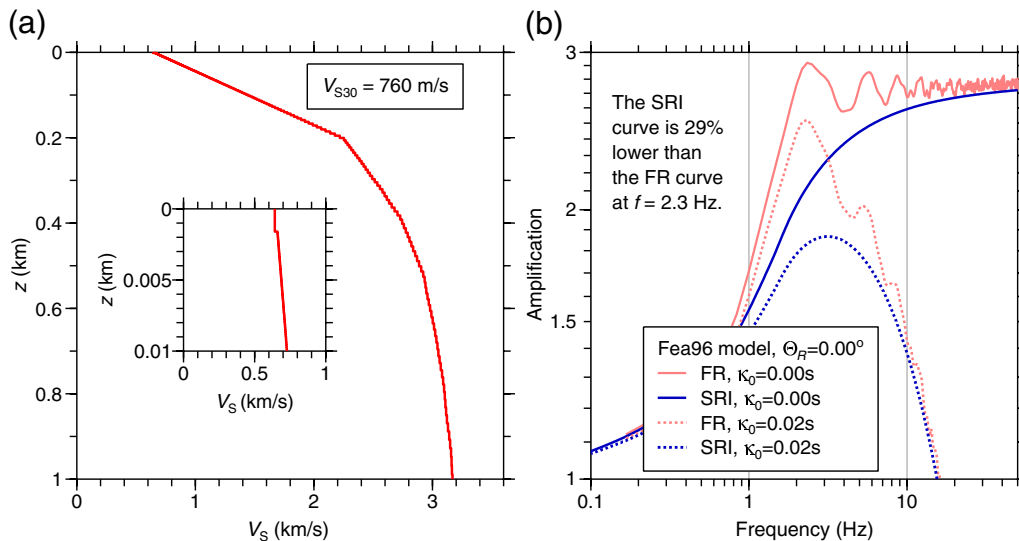


Figure 5. (a) Velocity profile used by Frankel *et al.* (1996; Fea96) for NEHRP class BC amplifications in eastern North America with inset, showing the shallow part of the model. (b) The amplification relative to the motion on the surface of a half-space with $V_S = 3.6$ km/s. The amplifications were computed using the SRI and FR calculations assuming plane SH waves, both with vertical incidence ($\Theta_R = 0^\circ$). The amplifications were computed with no attenuation ($\kappa_0 = 0.0$ s), and these amplifications were then multiplied by $\exp(-\pi\kappa_0 f)$, where $\kappa_0 = 0.02$ s. The color version of this figure is available only in the electronic edition.

computations), has a resonant frequency of 9.25 Hz. This model was not intended to represent a real model but only to act as an extreme example of a range of models having the same travel time from the surface to the bottom of the models.

Gradient Models: Frankel *et al.* (1996)

Frankel *et al.* (1996; Fea96) include a gradient velocity model for which $V_{S30} = 760$ m/s. This model was used with the SRI method by both Fea96 and Atkinson and Boore (2006; AB06) to derive amplifications for ground-motion simulations in eastern North America. Both studies accounted for attenuation by multiplying the amplifications by the factor in equation (3), for which Fea96 used $\kappa_0 = 0.01$ s and AB06 used $\kappa_0 = 0.02$ s. The velocity model used by the studies is shown in Figure 5a, and the SRI and FR amplifications without and with attenuation (with $\kappa_0 = 0.02$ s) are shown in Figure 5b. The attenuation responses are shown only to provide a guide to the frequencies for which the attenuation reduces the absolute level of the responses to such low levels that the differences in the FR and the SRI responses are of no consequence to ground-motion simulations. The oscillations in the FR amplifications for frequencies extending at least to 20 Hz are true features of the theoretical response of the gradient model, as they are virtually identical for models with 600 and 1200 layers. The SRI amplifications underestimate the FR amplifications over the entire range of frequencies, with a maximum reduction of 29% at 2.3 Hz. The amplifications from both methods tend to approach one another at high frequencies, although a persistent difference exists at high frequencies. This may be due to numerical limitations in the FR calculations, but any

reasonable attenuation makes these high frequency differences inconsequential for ground-motion simulations. More important are the differences in the SRI and FR amplifications for frequencies less than about 10 Hz (the frequency range of most engineering interest), for which the differences in the attenuated amplifications are noticeable even with the stronger of the two attenuation parameters used in the published applications (corresponding to $\kappa_0 = 0.02$ s).

Gradient Models: Boore and Joyner (1997)

Using a variety of observed shear-wave velocity models and inferences from compressional-velocity models, Boore and Joyner (1997; BJ97) proposed a model for a generic rock site in an active tectonic area. They used the SRI method to derive amplifications (commonly called “crustal amplifications” because they include amplifications of waves between a typical source depth of 8 km and the earth’s surface). The model and the amplifications derived from the model have been widely used, both by themselves (e.g., Atkinson and Silva, 2000; Campbell, 2003; Malagnini *et al.*, 2007; Ameri *et al.*, 2011; Graves and Aagaard, 2011; Ugruhan *et al.*, 2012) or as the basis for generating a suite of velocity models for a specified V_{S30} (Cotton *et al.*, 2006; see the Data and Resources section for a reference to notes containing a modification of their procedure). The velocity model and the amplifications for a vertical angle of incidence are shown in Figure 6. As in the previous example, there is a persistent underestimation of the amplifications from the SRI method compared to those from the FR calculations; in this case the reduction is 18% for a frequency of 2.6 Hz. There is a larger mismatch at a frequency of about 55 Hz (due to resonance in the 1 m thick top layer, as indicated in Fig. 6a), but any

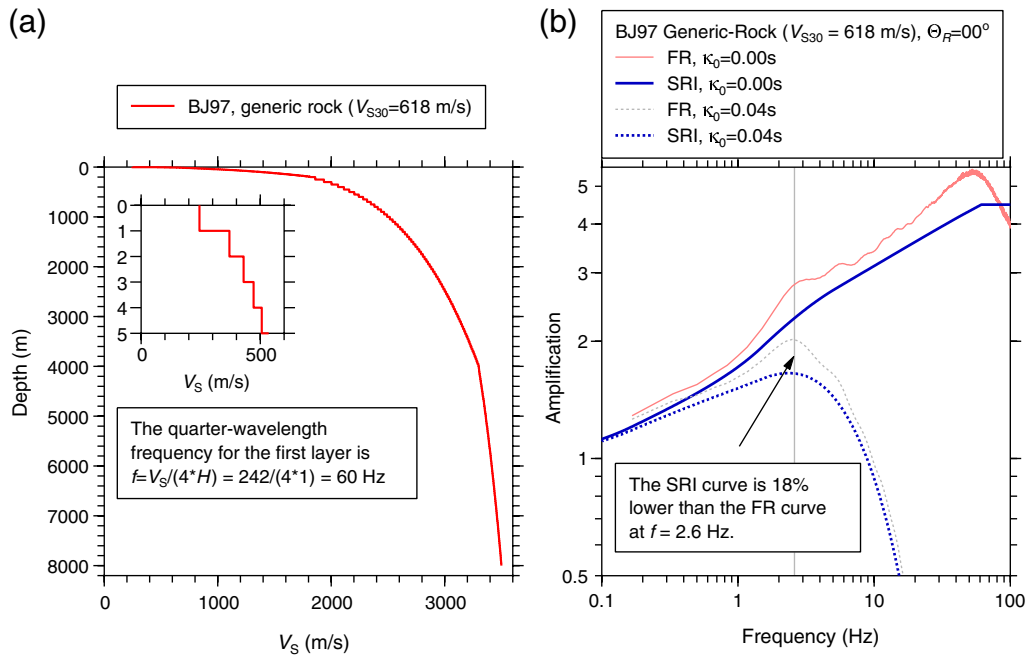


Figure 6. (a) The velocity profile used by Boore and Joyner (1997; BJ97) for generic rock in western North America. (b) The amplifications for the full profile, using two methods of calculation, with and without attenuation (see the caption for the previous figure for explanation). The densities used in the calculations were obtained from velocity–density relations given in *daves_notes_on_relativity_density_to_velocity_v1.2.pdf* (see the [Data and Resources](#) section). The color version of this figure is available only in the electronic edition.

reasonable attenuation (such as the typical value of $\kappa_0 = 0.04$ s used in Fig. 6) makes this mismatch of no importance for ground-motion simulation. (There is a difference in the κ_0 values used in this and the previous example because the former application was for eastern North America, where the average velocity is higher, and it is thought that the attenuation should be less than in tectonically active areas). The persistent underestimation of the amplifications by the SRI method for the BJ97 generic rock model is also shown in Poggi *et al.* (2011).

BJ97 computed SRI amplifications from the velocity model shown in Figure 6, and these amplifications have subsequently been adopted by many authors in their simulations of ground motions (see above references). The amplifications are shown in Figure 7 of BJ97 and are given in their table 3. A careful comparison of their Figure 7 with Figure 6 in this paper, however, reveals two obvious differences: (1) the amplifications at high frequencies are smaller in BJ97 than in Figure 5, and (2) more importantly, the comparison of the SRI and FR amplifications in figure 7 of BJ97 are better than those shown in Figure 6. The explanation for the difference in amplitudes at high frequencies is simple: The density model used in BJ97 assigned higher densities to lower shear-wave velocities than in more recent calculations (which use velocity–density relations given in some unpublished work by me; see the [Data and Resources](#) section). The apparently better comparison of the SRI and FR amplifications in BJ97 is due to erroneously comparing SRI amplifications at 0° angle of incidence with FR amplifications at 30°

and 45° angles of incidence in BJ97. The proper comparison is given in Figure 7.

Regarding the dependence of both types of amplification on the angle of incidence, I first point out that it is not clear what angle of incidence (or more properly, what takeoff angle) to use for waves leaving the source near 10 km in the crust, at least when the amplifications are used in the stochastic method, which attempts to capture complex physics with simple relations between a physical parameter and frequency. The actual surface motion is probably a mixture of waves leaving from a range of takeoff angles, the range depending on the epicentral distance and the crustal structure. But as the waves approach the surface, the angles of incidence should approach 0° (vertical incidence) because of refraction. To see the effect of this in the context of the SRI method, the left graph in Figure 8 shows the average angles of incidence for three takeoff angles plotted against frequency for the BJ97 generic rock model, for which the angles of incidence were calculated using the QWL velocities and equation (2). As expected, as frequency increases the averaging depth decreases, the average velocity thus decreases, and the waves are refracted more to the vertical. The consequence for the site amplification is shown in Figure 8b. Because $\bar{\Theta}$ is almost 0.0 for frequencies greater than about 1 Hz, the angle of incidence part of the amplification in equation (1) is controlled almost entirely by the takeoff angle Θ_R , and the amplifications become independent of frequency, with approximately constant differences

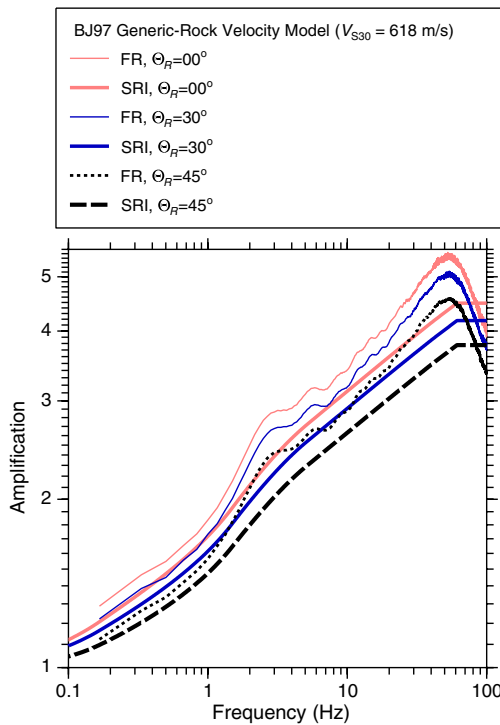


Figure 7. Amplifications computed in two ways for the velocity profile shown in Figure 6 for three takeoff angles from the source. There was no attenuation in the models. The color version of this figure is available only in the electronic edition.

dependent only on Θ_R . This is the explanation for the differences seen in Figure 7.

Combining Gradients and Step Changes in Impedance

In most of the previous examples, amplifications from the SRI method were close to an average of the FR amplifi-

cations for frequencies above the fundamental mode, when the velocity models contained a large change of impedance across a layer boundary. This was generally not the case for the gradient models, for which the SRI amplifications were systematically low over a wide frequency range (the power-law example in Fig. 4 being an exception). This raises the question of what would happen when a velocity model has a gradient over a portion of the model, with a large impedance contrast at some depth. Is it a general result that the SRI amplifications are an average of FR amplifications if a large impedance contrast exists in the model? I cannot answer this theoretically, and obviously I cannot explore the multitude of possible models with gradients and impedance contrasts. But in keeping with the use of a few models as examples in this paper, I modified the BJ97 generic rock model in Figure 6 by truncating it at 200 m with three half-spaces whose velocities were chosen to give a range of impedance changes across the interface. The modified models are shown in Figure 9a, and the resulting amplifications from both the SRI and the FR methods are shown in Figure 9b. The FR amplifications with no impedance change at 200 m form a lower bound of the amplifications with an impedance change, and as the size of the impedance change increases, the SRI amplifications approach the FR amplifications for frequencies greater than the fundamental mode. I also note that the first peaks in the FR amplifications occur at frequencies greater than the QWL frequency of 1.45 Hz corresponding to the bottom of the gradient portion of the model (a kink in the SRI amplifications occurs at this frequency); such a shift of the peak frequency also occurred in the examples in Figure 4, and is another example of how the peak frequency estimated by the simple rule-of-thumb equation given earlier, which replaces the actual

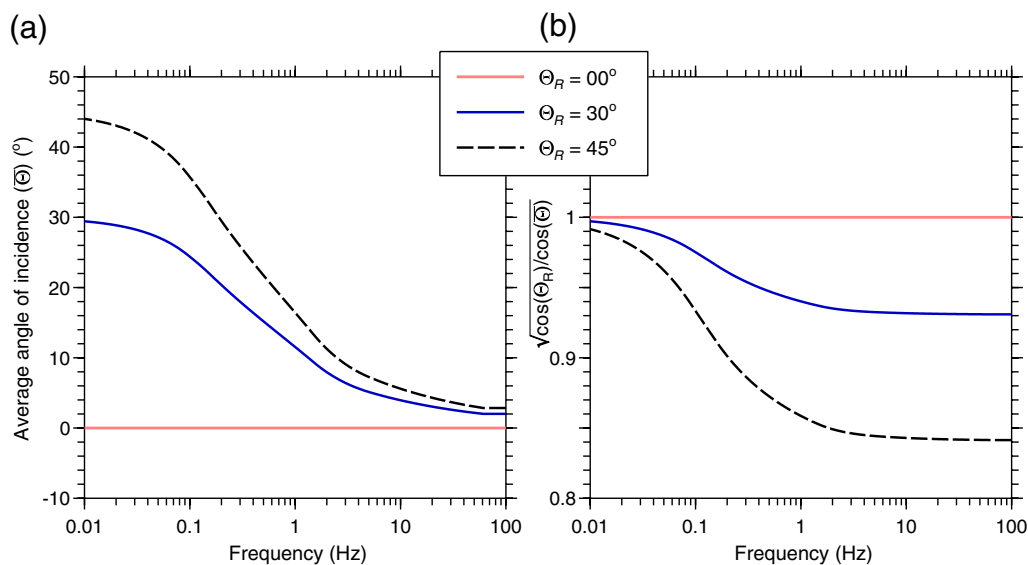


Figure 8. (a) Average angle of incidence versus frequency for three takeoff angles at the reference depth (Θ_R), for the model used in Figure 7. (b) The factor in the site amplification involving the angles of incidence. The color version of this figure is available only in the electronic edition.

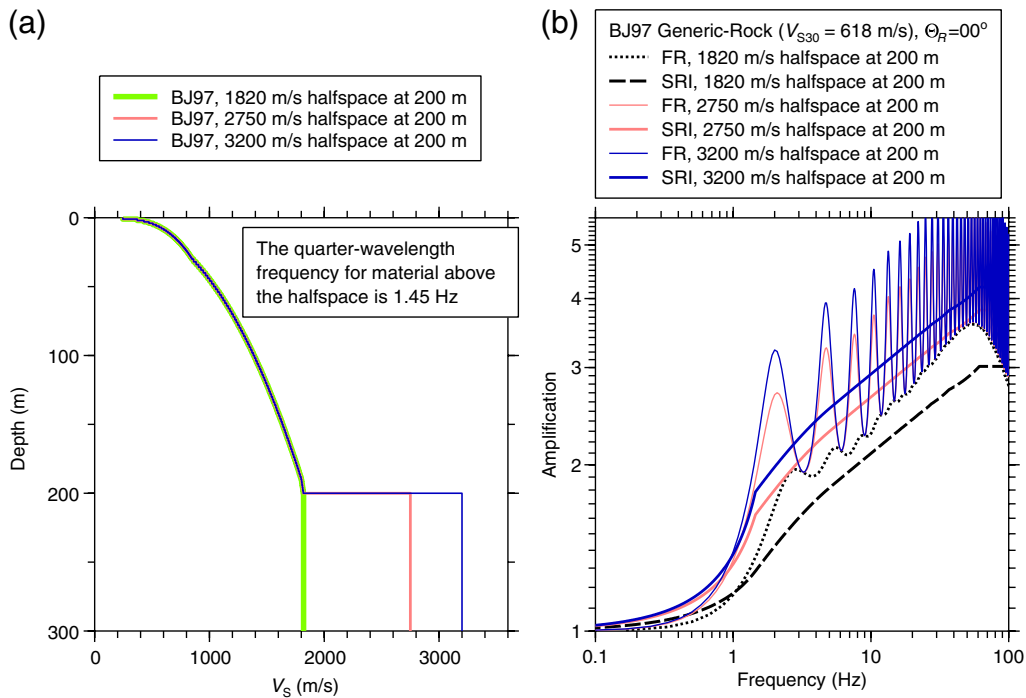


Figure 9. (a) The velocity profile used by Boore and Joyner (1997; BJ97) for generic rock in western North America, truncated at 200 m by constant-velocity half-spaces with velocities as indicated in the legend. (b) The amplifications for the three profiles shown in (a), using two methods of calculation. There was no attenuation in the models. The color version of this figure is available only in the electronic edition.

velocity model with a constant-velocity layer, can be misleading.

Including Attenuation in Site Response

The SRI method incorporates damping by multiplying the amplification given by equation (1) by the operator in equation (3). This is convenient because only one parameter is needed to specify the attenuation operator. In the SRI and FR comparisons in Figures 5 and 6, the simple attenuation operator was also applied to the FR amplifications, in which case the ratio of attenuation amplifications from the SRI and FR methods will be the same as the unattenuated amplifications. The only reason to show the attenuation response in those figures was to assess the frequencies for which the absolute level of the site response was reduced so much that any differences in the SRI and FR amplifications were of no consequence to predictions of ground motions of engineering interest. A more physical way of including attenuation in the FR calculations is to specify a damping parameter Q in each layer (e.g., Campbell, 2009). In Figure 10, I compare the attenuated FR responses using both methods of including attenuation. I also show the SRI site response in Figure 10. To highlight the effect of attenuation, the model is the simple one-layer model shown in Figure 3. I assume that Q is independent of frequency in this example; the κ_0 used in the calculations was given by the travel time through the layer divided by the corresponding Q . The most obvious difference in the FR response for the two ways of including attenu-

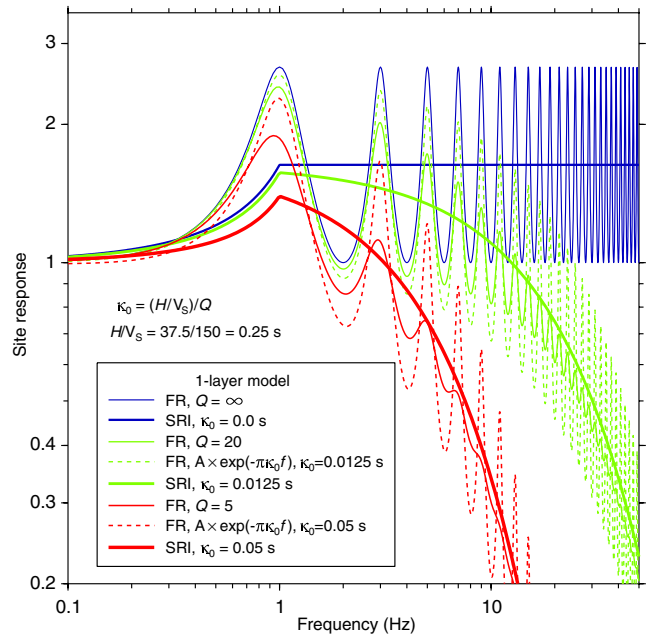


Figure 10. Effect of including attenuation in various ways: (1) as Q values in the layer for the FR calculations; and (2) by multiplying the undamped amplification by $\exp(-\pi\kappa_0 f)$, with $\kappa_0 = (H/V_S)/Q$ for the FR and the SRI calculations. For this model, $\kappa_0 = 0.0125$ s and 0.05 s, correspond to $Q = 20$ and 5 , respectively. The color version of this figure is available only in the electronic edition.

ation is that the FR response with finite Q in the layer becomes smoother with increasing frequency than when the attenuation is included by multiplying the unattenuated FR response with the attenuation operator in equation (3), in which case the peak-to-trough differences for all higher modes are retained. The difference in the total response is most likely explained by the operator in equation (3) assuming attenuation due to one passage across the layer, whereas the FR response is made up of the interference of multiple reverberations, so that the effective path length over which the waves are attenuated is greater than a single layer thickness. Two consequences of the increased attenuation from the use of Q in the layers are that the amplitude of the fundamental mode is reduced by about 20% for the strongest attenuation, $Q = 5$, and that the total response is about 10%–13% lower than the SRI response at frequencies greater than the fundamental-mode frequency. Both consequences suggest that the size of the persistent underestimation of the site response from the SRI method shown in the examples in this paper will be somewhat reduced if the full SRI response (amplification and attenuation) had been compared to the full FR response with attenuation accounted for by using a depth dependent Q . The more physical way of including the attenuation adds the complication of estimating depth dependent Q in the FR calculations, and because the difference in the full response is relatively small, I decided to base my comparisons on the unattenuated response instead.

Some Uses of the SRI Method

Crustal Amplification Functions

The most widespread use of the SRI method is probably in determining crustal amplification functions used in simulations of ground motions (e.g., [Boore and Joyner, 1997](#)). The velocity models used in these applications are generally characterized by gradients, with no significant impedance contrasts. As shown in this paper, the SRI amplifications consistently underestimate the FR amplifications for such models, over a wide range of frequencies. The underestimation is not large, however, being at most about 30%. In addition, it is not clear that the FR method, which assumes plane waves, should be used to calculate the amplification from the source depth of the earthquakes for which ground motions are simulated, to the surface (this is the crustal amplification used in the stochastic simulations). ([Ou and Herrmann, 1990](#), use synthetic full-wave simulations of a point source in a layered media to derive average values of the geometrical spreading, attenuation, and the combined effect of a frequency-independent amplification and radiation pattern, but it is not easy to separate the combined effects into the simple components needed for the usual implementation of the stochastic model.) For these reasons, I think that the SRI method is useful in estimating crustal amplifications used in forward calculations of ground motions. This is particularly true when the crustal amplifications from the SRI method are used to

infer source properties, such as seismic moment and stress parameter, from recordings, and these properties are then used in forward calculations of the ground motion (using all of the same model parameters as used in the inversion of the data). This is a consistent process in which any systematic bias in the crustal amplifications is offset in the inverse and forward processes, as long as the frequencies used in the inversion are similar to those in the forward predictions.

Comparing Velocity Profiles

Another use of the SRI method is in comparing the amplifications for different velocity models. In a number of studies, velocity models have been obtained by different investigators at the same site or at nearby sites. The traditional way of comparing these models is to show plots of velocity versus depth, but this is less useful than showing the ground-motion amplifications for the various models, as that is generally what matters in practice. The problem with using FR calculations for the amplification calculations is that the discretization of the models can lead to apparent peaks and troughs in the response that vary from one model to another, and ratios of the response can then fluctuate wildly (as demonstrated shortly), masking the underlying variation of the ratio with frequency. Of course, averages of the FR amplifications over frequency could be used before forming the ratios, but the SRI accomplishes the same thing more simply. Another advantage of the SRI amplifications is that the ratio of amplifications above a well-defined frequency are not dependent on the velocity structure below the smaller of the depths to the bottom of the two velocity models being compared. This is in contrast to the FR calculations, for which simply replacing the material below the maximum depths of the velocity models with a constant-velocity half-space can cause misleading results, unless there is a true large change in impedances at the bottom of the model or the velocity for a considerable range of depths below the bottom of the model is essentially constant (thus approximating a half-space). SRI amplifications have been used by a number of authors to compare velocity models (e.g., [Boore and Brown, 1998](#); [Brown et al., 2002](#); [Stephenson et al., 2005](#); [Cornou et al., 2007](#); [Boore and Asten, 2008](#)). Here I show results adapted from [Boore and Asten \(2008\)](#). Many independent determinations of velocity models were made in the Santa Clara Valley near San Jose, California, at William Street Park (WSP), 200 m from a site from which velocities were measured in a borehole to 300 m depth at the Coyote Creek Outdoor Classroom (CCOC). Results from a deeper borehole within the Santa Clara Valley were combined with other information to extend the velocity models at WSP and CCOC to deeper depths (see [Boore and Asten, 2008](#), for details). Figure 11 shows the velocity models at the two sites, and Figure 12 shows the amplifications and the ratio of amplifications for the models, computed using the SRI and the FR methods. The SRI results

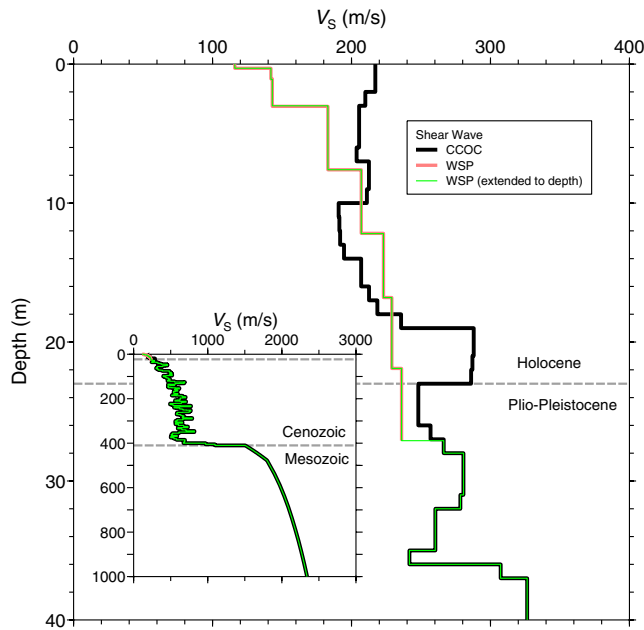


Figure 11. Velocity models from nearby sites (CCOC and WSP) near San Jose, California. The inset shows the models to 1000 m (see Boore and Asten, 2008, for details about the models). The color version of this figure is available only in the electronic edition.

are shown for models with and without the extension to depth; those results are the same for frequencies above 1.9 Hz, which correspond to the QWL frequency at the base of the WSP model (27.5 m), thus confirming the statements made earlier that the SRI amplifications above a well-defined frequency do not depend on the velocity structure beneath

the depth associated with that frequency. More important for the discussion in this section is the comparison of the ratios shown in Figure 12 for amplifications from the SRI and the FR methods; the latter oscillate rapidly, whereas the former have a smooth variation with frequency, from which I conclude that on average, the WSP velocity model will lead to larger amplifications than those from the CCOC model, with the difference increasing to more than a factor of 1.2 for frequencies above about 10 Hz.

Using QWL Velocities

An essential part of the SRI method introduced by Joyner *et al.* (1981) is the use of velocities averaged over a QWL in the amplification equation. As mentioned in the Introduction, the QWL velocities are useful outside of the SRI method. Joyner and Fumal (1985) developed GMPEs by using the frequency-dependent QWL velocity at a ground-motion recording site as the predictor variable for site response, and since then, V_{S30} has been used in numerous GMPEs (e.g., Boore *et al.*, 1994; Kanno *et al.*, 2006; Abrahamson *et al.*, 2008); it is being used in the current Pacific Earthquake Engineering Center Next Generation Attenuation-West 2 (PEER NGA-West2) project to update the previously published PEER NGA GMPEs for nonsubduction, active tectonic regions. With a view toward their use in GMPEs, Douglas *et al.* (2009) developed a method for generating velocity profiles from which QWL velocities and their uncertainties can be calculated. Poggi *et al.* (2011) showed that empirically determined frequency-dependent amplifications correlated with velocity averages to depths appropriate

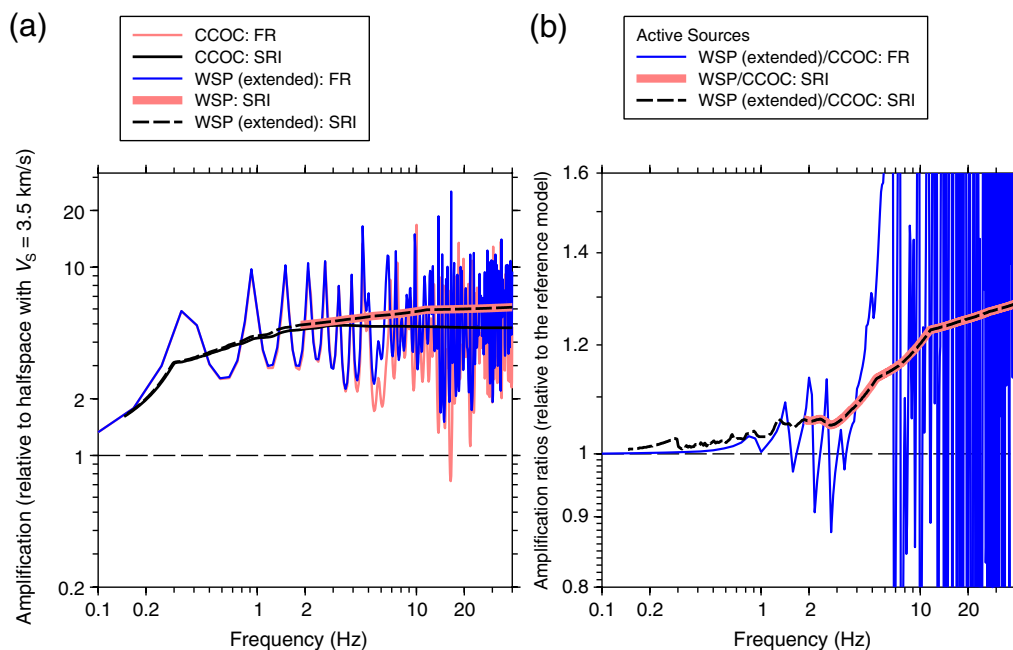


Figure 12. (a) Amplifications and (b) ratios of amplifications from the models at CCOC and WSP given in Figure 11 (modified from fig. 14 in Boore and Asten, 2008). The color version of this figure is available only in the electronic edition.

for the frequencies of the amplifications, and from this they inverted for a reference velocity model that produced an amplification of unity. They chose to use FR calculations in their inversion.

Conclusions

The SRI method has many advantages in calculating smoothed, approximate site amplifications for a wide variety of velocity models. The method is rapid, it does not depend on details of the velocity model, it associates a frequency of the amplification with each depth, and it smooths over the many peaks and troughs usually seen in theoretical FR calculations (these peaks and troughs are often not seen in average site-specific response calculated from real data, e.g., as shown by Thompson *et al.*, 2009). On the other hand, the SRI method consistently underestimates the peaks in resonant systems, and it underestimates the response of gradient models with no significant impedance contrasts, over a wide frequency range. For two gradient models used to develop crustal amplifications commonly employed in stochastic method ground-motion simulations, however, the underestimation is at most about 30%, which is comparable to uncertainties in a number of the parameters used in the simulations, and it is much smaller than typical uncertainties in observed ground motions. In addition, Thompson *et al.* (2011) find that site responses computed from the SRI method are in better agreement with observed site responses than those from the FR method. For these reasons, I recommend that the SRI method be used to develop site response functions for average velocity profiles. The underprediction of the SRI amplifications are not important for predictions of ground motions if those amplifications are used to derive source parameters such as the stress parameter controlling high frequency radiation, and those source parameters are then used with the SRI amplifications in forward predictions of ground motions. This is a consistent use of the model and any bias in the amplifications will largely cancel out.

Even though the SRI method is useful in many applications, the limitations demonstrated in this paper should be kept in mind, for there are certainly situations for which it is not appropriate. These situations include predicting the amplitude of the fundamental mode at a site when the local geology is such that a strong resonance independent of the azimuth of the incoming waves is expected, using the amplifications with source parameters that have not been derived using the same model, and using the method to predict amplifications when nonlinear site response is expected to be important.

Data and Resources

No data were used in this paper. The SRI and FR amplifications were computed using the programs *site_amp* and *nrattle*, respectively; they and various utility programs used in the computations are part of the SMSIM suite of programs,

available from the online software link at www.daveboore.com (last accessed 12 March 2013). *nrattle* is a modification by R. Herrmann of C. Mueller's program *rattle*; *nrattle* is included in the SMSIM suite of software with their permission. The densities used in some of the models were obtained from velocity–density relations given in *daves_notes_on_relatating_density_to_velocity_v1.2.pdf*, and the modification to the Cotton *et al.* (2006) procedure for generating velocity profiles is given in *daves_notes_on_interpolating_two_given_velocity_profiles_to_obtain_a_velocity_profile_with_specified_v30_v1.0.pdf*; both of these are available from www.daveboore.com/daves_notes.html (last accessed 12 March 2013). The figures were prepared using CoPlot (<http://www.cohort.com>, last accessed 23 April 2013).

Acknowledgments

I thank Sinan Akkar and Frank Scherbaum for providing references and background material that I used in preparing this paper, and Jack Boatwright, Ken Campbell, John Douglas, Valerio Poggi, and an anonymous reviewer for reviews of this article.

References

- Abrahamson, N., G. Atkinson, D. Boore, Y. Bozorgnia, K. Campbell, B. Chiou, I. M. Idriss, W. Silva, and R. Youngs (2008). Comparisons of the NGA ground-motion relations, *Earthq. Spectra* **24**, 45–66.
- Aki, K., and P. G. Richards (2002). *Quantitative Seismology*, Second Ed., University Science Books, Sausalito, California, 700 pp.
- Ameri, G., A. Emolo, F. Pacor, and F. Gallovič (2011). Ground-motion simulations for the 1980 *M* 6.9 Irpinia earthquake (southern Italy) and scenario events, *Bull. Seismol. Soc. Am.* **101**, 1136–1151.
- Anderson, J. G., Y. Lee, Y. Zeng, and S. Day (1996). Control of strong motion by the upper 30 meters, *Bull. Seismol. Soc. Am.* **86**, 1749–1759.
- Atkinson, G. M., and D. M. Boore (2006). Earthquake ground-motion prediction equations for eastern North America, *Bull. Seismol. Soc. Am.* **96**, 2181–2205.
- Atkinson, G. M., and W. Silva (2000). Stochastic modeling of California ground motions, *Bull. Seismol. Soc. Am.* **90**, 255–274.
- Boore, D. M. (2003). Prediction of ground motion using the stochastic method, *Pure Appl. Geophys.* **160**, 635–676.
- Boore, D. M. (2004). Can site response be predicted? *J. Earthq. Eng.* **8**, no. 1, 1–41 (special issue).
- Boore, D. M., and M. W. Asten (2008). Comparisons of shear-wave slowness in the Santa Clara Valley, California, from blind interpretations of data from a comprehensive set of invasive and non-invasive methods using active- and passive-sources, *Bull. Seismol. Soc. Am.* **98**, 1983–2003.
- Boore, D. M., and L. T. Brown (1998). Comparing shear-wave velocity profiles from inversion of surface-wave phase velocities with downhole measurements: Systematic differences between the CXW method and downhole measurements at six USC strong-motion sites, *Seismol. Res. Lett.* **69**, 222–229.
- Boore, D. M., and W. B. Joyner (1991). Estimation of ground motion at deep-soil sites in eastern North America, *Bull. Seismol. Soc. Am.* **81**, 2167–2185.
- Boore, D. M., and W. B. Joyner (1997). Site amplifications for generic rock sites, *Bull. Seismol. Soc. Am.* **87**, 327–341.
- Boore, D. M., W. B. Joyner, and T. E. Fumal (1994). Estimation of response spectra and peak accelerations from western North American earthquakes: An interim report, Part 2, *U.S. Geol. Surv. Open-File Rept.* 94-127, 40 pp.

- Boore, D. M., E. M. Thompson, and H. Cadet (2011). Regional correlations of V_{S30} and velocities averaged over depths less than and greater than 30 m, *Bull. Seismol. Soc. Am.* **101**, 3046–3059.
- Brown, L. T., D. M. Boore, and K. H. Stokoe (2002). Comparison of shear-wave slowness profiles at ten strong-motion sites from non-invasive SASW measurements and measurements made in boreholes, *Bull. Seismol. Soc. Am.* **92**, 3116–3133.
- Campbell, K. W. (2003). Prediction of strong ground motion using the hybrid empirical method and its use in the development of ground-motion (attenuation) relations in eastern North America, *Bull. Seismol. Soc. Am.* **93**, 1012–1033.
- Campbell, K. W. (2009). Estimates of shear-wave Q and κ_0 for unconsolidated and semiconsolidated sediments in eastern North America, *Bull. Seismol. Soc. Am.* **99**, 2365–2392.
- Cornou, C., M. Ohrnberger, D. M. Boore, K. Kudo, and P.-Y. Bard (2007). Derivation of structural models from ambient vibration array recordings: Results from an international blind test, in *Third International Symposium on the Effects of Surface Geology on Seismic Motion*, P.-Y. Bard, E. Chaljub, C. Cornou, F. Cotton, and P. Gueguen (Editors), Grenoble, France, 30 August–1 September 2006, Laboratoire Central des Ponts et Chaussées.
- Cotton, F., F. Scherbaum, J. J. Bommer, and H. Bungum (2006). Criteria for selecting and adjusting ground-motion models for specific target regions: Application to central Europe and rock sites, *J. Seismol.* **10**, 137–156.
- Day, S. M. (1996). RMS response of a one-dimensional halfspace to SH , *Bull. Seismol. Soc. Am.* **96**, 363–370.
- Douglas, J., P. Gehl, L. F. Bonilla, O. Scotti, J. Régnier, A.-M. Duval, and E. Bertrand (2009). Making the most of available site information for empirical ground-motion prediction, *Bull. Seismol. Soc. Am.* **99**, 1502–1520.
- Frankel, A., C. Mueller, T. Barnhard, D. Perkins, E. Leyendecker, N. Dickman, S. Hanson, and M. Hopper (1996). National seismic hazard maps: Documentation June 1996, *U.S. Geol. Surv. Open-File Rept. 96-532*, 69 pp.
- Graves, R. W., and B. T. Aagaard (2011). Testing long-period ground-motion simulations of scenario earthquakes using the M_w 7.2 El Mayor-Cucapah mainshock: Evaluation of finite-fault rupture characterization and 3d seismic velocity models, *Bull. Seismol. Soc. Am.* **101**, 895–907.
- Joyner, W. B., and T. E. Fumal (1984). Use of measured shear-wave velocity for predicting geologic site effects on strong ground motion, in *Proc. Eighth World Conf. on Earthquake Eng.*, San Francisco, Vol. 2, 777–783.
- Joyner, W. B., and T. E. Fumal (1985). Predictive mapping of earthquake ground motion, in *Evaluating Earthquake Hazards in the Los Angeles Region*, J. I. Ziony (Editor), *U.S. Geol. Surv. Profess. Paper 1360*, 203–220.
- Joyner, W. B., R. E. Warrick, and T. E. Fumal (1981). The effect of Quaternary alluvium on strong ground motion in the Coyote Lake, California, earthquake of 1979, *Bull. Seismol. Soc. Am.* **71**, 1333–1349.
- Kanno, T., A. Narita, N. Morikawa, H. Fujiwara, and Y. Fukushima (2006). A new attenuation relation for strong ground motion in Japan based on recorded data, *Bull. Seismol. Soc. Am.* **96**, 879–897.
- Malagnini, L., K. Mayeda, R. Uhrhammer, A. Akinci, and R. B. Herrmann (2007). A regional ground-motion excitation/attenuation model for the San Francisco region, *Bull. Seismol. Soc. Am.* **97**, 843–862.
- Ou, G.-B., and R. B. Herrmann (1990). A statistical model for ground motion produced by earthquakes at local and regional distances, *Bull. Seismol. Soc. Am.* **80**, 1397–1417.
- Poggi, V., B. Edwards, and D. Fäh (2011). Derivation of a reference shear-wave velocity model from empirical site amplification, *Bull. Seismol. Soc. Am.* **101**, 258–274.
- Stephenson, W. J., J. N. Louie, S. Pullammanappallil, R. A. Williams, and J. K. Odum (2005). Blind shear-wave velocity comparison of ReMi and MASW results with boreholes to 200 m in Santa Clara Valley: Implications for earthquake ground-motion assessment, *Bull. Seismol. Soc. Am.* **95**, 2506–2516.
- Thompson, E. M., L. G. Baise, R. E. Kayen, and B. B. Guzina (2009). Impediments to predicting site response: Seismic property estimation and modeling simplifications, *Bull. Seismol. Soc. Am.* **99**, 2927–2949.
- Thompson, E. M., L. G. Baise, R. E. Kayen, E. C. Morgan, and J. Kaklamanos (2011). Multiscale site-response mapping: A case study of Parkfield, California, *Bull. Seismol. Soc. Am.* **101**, 1081–1100.
- Ugurhan, B., A. Aysegul, A. Akinci, and L. Malagnini (2012). Strong-ground-motion simulation of the 6 April 2009 L'Aquila, Italy, earthquake, *Bull. Seismol. Soc. Am.* **102**, 1429–1445.
- Wiggins, J. H., Jr. (1964). Effect of site conditions on earthquake intensity, *Proc. Am. Soc. Civil Eng. J. Structural Div.* **90**, no. ST2, 279–313.

U.S. Geological Survey
MS 977, 345 Middlefield Road
Menlo Park, California 94025
boore@usgs.gov

Manuscript received 20 September 2012